Journal of Materials Chemistry B

RSC Publishing

PAPER

View Article Online
View Journal | View Issue

Cite this: J. Mater. Chem. B, 2013, 1, 2724

E. coli–quantum dot bioconjugates as whole-cell fluorescent reporters for probing cellular damage†

Raghuraj S. Chouhan, Javed H. Niazi* and Anjum Qureshi*

Received 11th March 2013
Accepted 3rd April 2013

DOI: 10.1039/c3tb20338g

www.rsc.org/MaterialsB

A quantum dot (QD) conjugated whole-cell *E. coli* biosensor (*E. coli*–QD bioconjugates) was developed as a new molecular tool for probing cellular damage. The *E. coli*–QD bioconjugates were viable and exhibited fluorescence emission at 585 nm. Scanning electron microscopy (SEM) analysis of *E. coli*–QD bioconjugates revealed that the QDs were immobilized on the cell-surfaces and the fluorescence emission from QDs present on cell-surfaces was visualized by confocal microscopic examination. The *E. coli*–QD bioconjugates were employed as whole-cell fluorescent reporters that were designed to function as fluorescence switches that turn-off when cellular damage occurs. In this study, multi-walled carbon nanotubes (CNTs) were utilized as a model nanomaterial to probe cellular damage. Fluorescence spectra were recorded after the exposure of *E. coli*–QD bioconjugates with CNTs. We observed a strong correlation between fluorescence emission spectra, SEM and confocal microscopic analysis demonstrating that CNTs induced a dose and exposure time-dependent cellular toxicity. This toxicity mainly occurred by the physical interaction and cellular trafficking mechanisms that led to the collapse of the cellular structure and thus loss of fluorescence. The responses of *E. coli*–QD bioconjugates against CNTs were also visualized by simply exposing the cells to UV light and therefore rapid toxicity analysis and screening can be made. Our study demonstrated an easy and simple method to determine an important mechanistic perspective for the biological toxicity of chemicals or nanomaterials (NMs).

Introduction

Semiconductor QDs are luminescent inorganic NMs that exhibit unique optical properties, such as broad excitation spectra, size dependent emission profiles, and long fluorescence lifetime. The unique optical properties of QDs make them appealing as *in vivo* and *in vitro* fluorophores in a variety of biological investigations, in which traditional fluorescent labels based on organic molecules fail to provide long-term stability and simultaneous detection of multiple signals. Due to such unique properties, QDs have attracted great interest as labeling probes in biological and biomedical applications. QDs as labeling probes have been successfully used in fluorescent resonance energy transfer (FRET),[1,2] *in vitro* and *in vivo* imaging,[3–5] immunoassays[6,7] and DNA hybridization.[8] Hence, bioconjugation of QDs is of great importance in biological applications.[9] So far, commonly used approaches for conjugation of biomolecules to QDs are mainly based on covalent cross-linking,[8,10–13] electrostatic binding,[14,15] non-covalent biotinavidin binding,[16] hydrophobic attraction[16] and nickel-based histidine tagging.[3] Covalent conjugation of QDs is the most commonly used approach, which is based on the cross-linking reaction between amine and carboxyl groups in the presence of carbodiimide as a catalyst,[4,6,12] as well as, the cross-linking reaction between amine and sulfhydryl groups in the presence of maleimide as a catalyst.[6] The carboxylated QDs have been conjugated to the amino groups of biomolecules such as proteins, enzymes, and antibodies.[17] This linking approach is simple and cheap, and currently, it is widely used in certain biosystems. In order to improve the conjugation efficiency, surface charge states of proteins and QDs were adjusted by chemical modification of proteins[16] and surface modification of QDs. However, QDs labeling on whole-cells while keeping the cells alive is scarce, which provides great potential to use them as whole-cell fluorescence reporters for assessing toxicological impacts on cells.

Currently, over 500 consumer products in the market claim to contain elements of nanoscience and nanotechnology with new entries coming daily.[18] This market annually requires metric tons of raw NMs, ranging from nano-sized metals and metal oxide particles to carbon nanotubes.[19,20] The demand for nanotechnology in medical products will be expected to reach $18 billion in 2014.[18] Such manufacturing and consumer utilization then produces multiple different sources of release of these materials into the environment, eco-system, water[21] and

Sabanci University Nanotechnology Research and Application Center, Orta Mah., Tuzla, 34956, Istanbul, Turkey. E-mail: javed@sabanciuniv.edu; anjum@sabanciuniv.edu; Fax: +90 216 483 9885; Tel: +90 216 483 9879; +90 216 483 9000/2441

† Electronic supplementary information (ESI) available: Fig. S1–S3 for responses of bioconjugates to CNTs at different time intervals. See DOI: 10.1039/c3tb20338g

food supplies, and other routes of non-voluntary entry into the human body.[20–22] Therefore, toxicity and risk assessments of engineered nanomaterials (ENMs) are receiving much attention because of the following reasons: (a) increased use of NMs and commercialization of nanotechnology products, (b) exposure of NMs in the environment and humans, (c) NMs can be tailored according to the desired characteristics for different applications such as consumer products, biomarkers, biosensors and catalysts and these modifications in NMs may be hazardous to human health and the environment and (d) currently, a complete understanding of the interactions of nanostructures with biological systems is lacking and thus it is unclear whether the exposure of humans, animals, insects and plants to engineered nanostructures could produce harmful biological responses.

Bacterial cells can be an ideal choice as biological recognition elements because they (a) grow rapidly and (b) respond to external stress (stimuli), such as toxic chemicals that lead to altered cellular dynamics, including metabolism, growth and cell surface charge distribution. Such responses can be utilized to predict the toxicity impacts of chemicals on other living cells.[23,24] The toxicity response of bacterial cells is often determined in terms of stress responses that are imposed by chemicals, such as CNTs. The stress responses in bacteria primarily begin at the cell-surface, cell-wall or membrane. However, the results from cytotoxicity studies with CNTs and other NMs are often contradictory, likely because of the use of CNTs of different sizes, purities and functionalizations,[25] different cell culture media[26] and use of a variety of cell types.[27] Such observations underscore the need for simple methods to test toxicity of NMs on living cells.[28]

Here, we have developed a bioassay that utilized viable *E. coli* whole-cells as baits to determine the cellular damage induced by CNTs as a model NM. It required labeling of cells in order to probe their responses against CNTs in the form of detectable signals. Labeling of cells was done by non-toxic chromogenic water-soluble, capped QDs that emit light or attain fluorescent abilities while cells are active and viable. Our results demonstrate that the *E. coli*–QD bioconjugates served as fluorescent switches that turn-off when CNTs interacted and damaged the cells. Our results also showed a strong correlation between the fluorescence emission spectra of CNTs exposed *E. coli*–QD bioconjugates and their morphological changes as determined by scanning electron microscopy (SEM). To our knowledge, there are no reports associated with the use of viable *E. coli*–QD bioconjugates to probe the interaction of NMs. Therefore, the assay developed in this study has a great potential to be applied as a tool for screening of various other NMs, toxic chemicals, drugs, food samples and environmental contaminants.

Experimental

Chemicals and reagents

The wild-type *E. coli* DH5α strain was used as a model living bacterial cell in this study. Luria–Bertani broth (LB-broth) and Luria–Bertani agar (LB-agar) were obtained from Difco (MI, USA). *N*-Hydroxysuccinimide (NHS) and *N*-ethyl-*N*′-(3-(dimethylamino) propyl)carbodiimide (EDC) were purchased from Sigma-Aldrich and multiwalled carbon nanotubes (CNTs) were obtained from Arry® International Group Ltd (Germany) with a diameter of 10–20 nm, purity of >95 wt%, and were ~20 μm long. Triton-X 100 was procured from Merck, Germany. A 10 mM Phosphate Buffer Saline (PBS), pH-7.4 used in this study was prepared from a 10× stock solution accordingly and prepared with deionized water (Milli Q, Millipore, Barnstead, CA, USA). Qdot® 585 ITK™ carboxyl quantum dots (Invitrogen) were used as labeling probes having an emission maximum at ~585 nm. All other reagents used were of analytical grade.

Apparatus

All glassware and solutions used in this study prior to the experiment were autoclaved with HMC, Hirayama autoclave, Che Scientific Co., Hong Kong. All bioconjugation studies and related work were carried out in a Thermo Scientific HERAsafe® KS microbiological safety cabinet. The spectral studies of the *E. coli*–QD bioconjugate and different stress induced chemicals were done in a range of 500 nm to 750 nm with advanced NanoDrop 3300 Fluorospectrometer (Thermo Scientific NanoDrop Products). Scanning electron microscopy (SEM) images were taken with a Hitachi S-4700 Field Emission Scanning Electron Microscope (Japan). All optical measurements were performed at room temperature under ambient conditions.

Preparation of the *E. coli* culture

Lyophilized cells of *E. coli* DH5α were precultured in LB-broth at 37 °C for 15 h and then the cells were harvested by centrifugation at 3000 rpm for 5 min at 4 °C. The cells were subsequently washed thrice with sterile PBS followed by centrifugation for 5 min at 3000 rpm at 4 °C. The cell pellet was suspended in PBS and colony forming units (CFUs) were measured by serial dilution followed by plating on LB-agar plates. The cell-suspension was divided into several aliquots carrying the same number of cells (~10^9 CFU mL^{-1}) for test and control experiments.

Ex vivo labeling of *E. coli* cells with QDs

A two-step protocol was employed for the *ex vivo* labeling of *E. coli* cells with carboxyl QDs (cat. no. Q21311MP) as shown in Scheme 1. The QDs chosen in this study had emission around 585 nm and more brightly fluoresce under an ultraviolet lamp. Here, free –COOH groups of QDs and primary amine-containing bio-molecules on *E. coli* cell-surface were covalently coupled by using a modified previously reported method.[29] In brief, freshly obtained *E. coli* cell pellets were resuspended in 100 μL of PBS, pH-7.4 containing a mixture of 50 mM EDC and 5 mM NHS and incubated for 5 min at 25 °C. This mixture was quickly added with 2 μL of 8 mM QD_{585} solution and the entire reaction mixture was incubated again at 25 °C for 15 min under constant shaking at 110 rpm. The QD-conjugated cell-suspension (*E. coli*–QD bioconjugates) was centrifuged at 1500 rpm for 3 min and the supernatant was removed and the pellet was washed thrice after resuspending in PBS, pH 7.4 followed by centrifugation with the same buffer and stored at 4 °C until use.

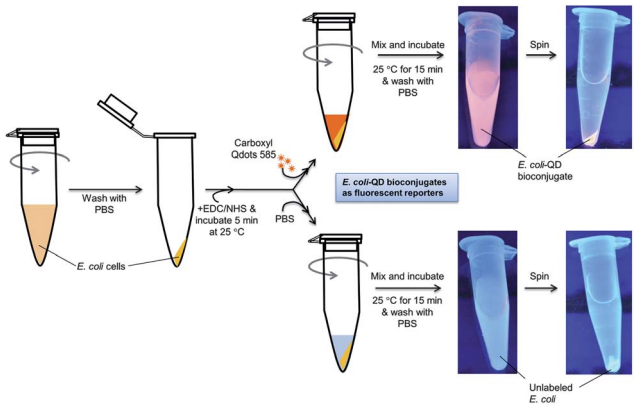

Scheme 1 *Ex vivo* labeling of *E. coli* cells with carboxy Qdot® 585 ITK™ by EDC/NHS coupling. Labeled and unlabeled cells were confirmed by exposing to UV light (302 nm).

The extent of conjugation was monitored using a NanoDrop Fluorospectrometer. Cell viability tests were carried out after appropriate dilutions with PBS followed by plating on LB-agar plates. CFUs were counted to ensure that no loss of cell viability occurred after the bioconjugation as well as to determine the shelf-life. The bioconjugates were stable for at least 2 months without the loss of cell viability. However, the QD-labeled cells once exposed to UV light tend to lose their viability as the number of CFUs declined to ~10% of the initial number. Therefore, bioconjugates that were once exposed to UV were not utilized for further experiments in this study.

Treatment of *E. coli*–QD bioconjugates with CNTs

All reagents used in this study were freshly prepared on the same day of the experiment. An aqueous stock CNT suspension (200 μL of 1 mg mL^{-1} in PBS, pH 7.4) containing Tween (0.1%) was sonicated with alternating cycles of 10 s pulse with an interval of 10 s for a total of 5 min using an ultrasonicator probe (Vibracell 75043). The thus obtained homogeneous CNT-stock suspension was quickly diluted to final concentrations of 0.1, 1 and 100 ng mL^{-1} CNTs in the same buffer, and this suspension was mixed with aliquots of *E. coli*–QD bioconjugates. The *E. coli*–QD bioconjugates and CNT mixture were incubated at different time intervals (1–3 h). For controls, except CNTs, all other conditions were identical (PBS was added in place of CNT suspension). Fluorescence emission spectra were recorded at each interval to probe the changes that occur before and after the treatment processes. All experiments were carried out in at least five replicates. The application of white light emitting diodes (LEDs) in the NanoDrop fluorospectrometer enabled scanning across a wide range of wavelengths covering 400–750 nm using sample volumes as low as 1–2 μL without cuvettes.

Rapid slide test for fluorescence emission

A rapid test was developed to qualitatively determine the responses of *E. coli*–QD bioconjugates against CNTs. Microscope glass slides were spotted with *E. coli*–QD bioconjugate suspension in PBS, pH 7.4. Each spot contained 25 μL volume of the above cell-suspension that accommodated 5 spots on each glass slide for rapid analysis against different concentrations of CNTs. The slides were directly visualized for fluorescence emission after exposing them to UV light (302 nm) using a UV transilluminator (BIO-RAD).

SEM analysis for morphology changes in *E. coli*–QD bioconjugates

The morphological changes of *E. coli*–QD bioconjugates caused by CNTs were investigated by SEM. The effective concentration of each sample was taken after 1–3 h incubation and the untreated controls were prepared both in standard and in salt free medium. A pre-cleaned silica chip with an area of 2 × 2 cm^2 was used for the sample analysis.[30] The samples were mounted on these chips and allowed to dehydrate at room temperature before taking the SEM images. The images were collected using a LEO Supra 35VP Scanning Electron Microscope.

Confocal microscopic examination of *E. coli*–QD bioconjugates

Fluorescence microscopy images were acquired with a Carl-Zeiss LSM 710 confocal microscope equipped with a Plan-Apochromat 63×/1.40 oil objective. QDs on cell-surfaces were excited with a 405 nm laser and images were collected using a 553–718 nm filter.

Results and discussion

Bioconjugation of QDs with viable *E. coli* cells

E. coli (DH5α) cells were covalently conjugated with carboxyl-QDs by EDC/NHS coupling. These *E. coli*–QD bioconjugates were separated from free QDs by centrifugation and fluorescence emission spectra were recorded that exhibited a characteristic fluorescent emission peak at 585 nm, which was derived from the cell-bound QDs (Fig. 1). Internal labeling of *E. coli* with

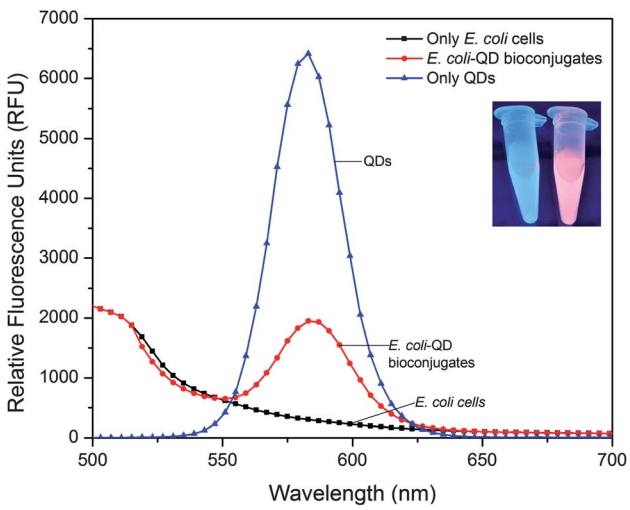

Fig. 1 Fluorescence emission spectra of pure QD_{585} (blue), *E. coli* (black) and *E. coli*–QD bioconjugates (red). The inset figure shows normal and QD-conjugated cells in suspension. The conjugated cells exhibit fluorescence emission property under UV light.

QDs by first permeabilizing the cells to uptake QDs has been reported, which may severely affect the integrity of cells.[31] Therefore, we employed here a covalent coupling strategy to immobilize QDs on the surface of the cells without affecting the cellular integrity or viability. The fluorescence nature of cells was also visualized simply with a brief exposure of a separate aliquot of *E. coli*–QD bioconjugates under UV light (Fig. 1 inset). It is noted that cells once exposed to UV light were more prone to lose their viability, and therefore, such cells were not utilized in this study as biological reporters.

The spectral features of *E. coli*–QD bioconjugates can be easily distinguished from the free QDs based on the appearance of a combination of (i) a shoulder peak at ~520 nm and (ii) a fluorescent peak at 585 nm as shown in Fig. 1 and ESI Fig. S1.† SEM analysis of bioconjugates revealed the presence of QDs on *E. coli* cell surfaces when compared to controls (Fig. 2a and b).

QDs of similar nature have been previously utilized in a variety of live-cell *in vitro* labeling experiments and no toxicity with such QDs is found with cells in culture.[32] QDs used in this study were made of a CdSe core encapsulated in a crystalline shell of ZnS followed by a coating with an amphophilic polymer. This coating prevents the release of free Cd and therefore QDs can be non-toxic to cells. However, SEM images taken soon after the bioconjugation process showed noticeable morphological changes when compared to the control cells (Fig. 2a and b). This morphology change was probably due to the release of urea as a by-product after the cell-treatment with EDC during the coupling reaction. Release of urea may have a reversible effect on cells that was recovered quickly after washing QD-bioconjugated cells with excess isotonic PBS solution. Further, coupling reaction was carried out with no contaminating –COOH groups other than those present on QDs in isotonic buffer that prevented undesirable polymerization on the cell-surface which can be detrimental to the cells. We subjected *E. coli*–QD bioconjugates to viability tests by plating them on LB-agar plates. It is clear from Fig. S2† that the cells actively grow in the LB-medium while the QDs were lost during the growth because the newly grown cells failed to exhibit fluorescence emission upon UV light exposure.

Confocal microscopic examination of *E. coli*–QD bioconjugates

The fluorescence light emitted from the cells in confocal images was predominantly seen at the terminal regions of individual cells and at the juncture of cell aggregates (Fig. 3a and b). Therefore QDs in *E. coli*–QD bioconjugates were found to be attached on the cell-surfaces to unknown biomolecules. Fig. 3c shows confocal images of *E. coli*–QD bioconjugates incubated with CNTs that formed heterostructures despite their poorly controllable degree of clustering, or surface coverage on the cells. We here observed a significant loss of fluorescence emission with CNT–*E. coli*–QD heterostructures. Quenching of photoluminescence occurred with CNTs and *E. coli*–QD bioconjugates when they assembled directly on the cell-surfaces forming QD–CNT composites.[33] This loss of fluorescence can be attributed to either or both of the following possibilities: (a) direct quenching effects of QDs upon interaction with CNTs as heterostructures and (b) cellular damage that may occur due to the interaction of cells with CNTs that release bound QDs. Both of these possibilities indicated that cells and CNTs have affinity to interact with each other mostly through non-covalent forces. Therefore, the *E. coli*–QD bioconjugates were used as a model living whole-cell biosensor to probe the interaction of CNTs.

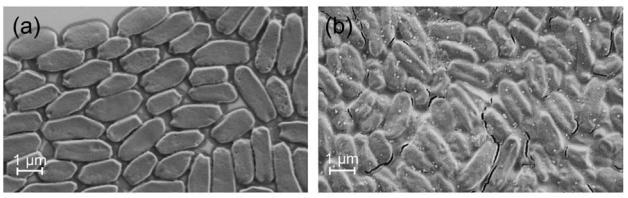

Fig. 2 Scanning electron microscopic images of (a) normal and (b) QD-conjugated *E. coli* cells.

E. coli–QD bioconjugates as fluorescent reporters for cellular perturbations

E. coli–QD bioconjugates were used as whole-cell fluorescence reporters for cellular damage. The cellular interactions, toxicity or damage that occurred to the *E. coli*–QD bioconjugates was determined by exposing CNTs as a model nanomaterial. The effect of various concentrations of CNTs (0.1–100 ng mL^{-1}) on cells was studied through changes in fluorescent characteristics of bioconjugates. Treatment of bioconjugates with initial 0.1 and 1 ng mL^{-1} CNT concentrations resulted in a concentration dependent diminishing response of their characteristic fluorescent peak at 585 nm (Fig. 4a). The fluorescence emission was also found to diminish with time (1–3 h) indicating that physical interaction or rupturing effects of CNTs on cells occurred that not only depended on concentration, but also on the exposure time (Fig. 4b, S3 and S4†). A higher concentration of CNTs (100 ng mL^{-1}) severely damaged the cells within 1 h of exposure (Fig. 4a) which was evidenced by a 150-fold loss of fluorescence emission at 585 nm (RFU = 10) within 1 h compared to the control *E. coli*–QD bioconjugates (untreated, RFU = 1500). Incubation of bioconjugates for 1 h with a higher CNT concentration (1 ng mL^{-1}) had a similar effect with a lower CNT concentration (0.1 ng mL^{-1}) incubated for 2 h (ESI Fig. S3†). This result indicated that proliferation and contact time (incubation time) with CNTs and *E. coli* cells severely affected the cellular integrity and thus irreversibly damaged the cells.

SEM images of *E. coli*–QD bioconjugates were taken in their free forms and after incubation with CNTs at different time intervals (Fig. 5a–d). We observed a strong correlation between fluorescent spectra and morphological pattern change by SEM analysis that demonstrated cytotoxic effects of CNTs on *E. coli*–QD bioconjugates (Fig. 4a and b and Fig. 5a–d). The cylindrical shape and high aspect ratio of CNTs allow their penetration through the membrane, similar to a 'nanosyringe', which has been experimentally studied[34] and theoretically simulated.[35] *E. coli* cells were affected more in direct contact and in suspended aggregates with CNTs and loss of viability was up to 80% at the initial exposure.[36] The diminished fluorescence emission of *E. coli*–QD bioconjugates was therefore attributed to

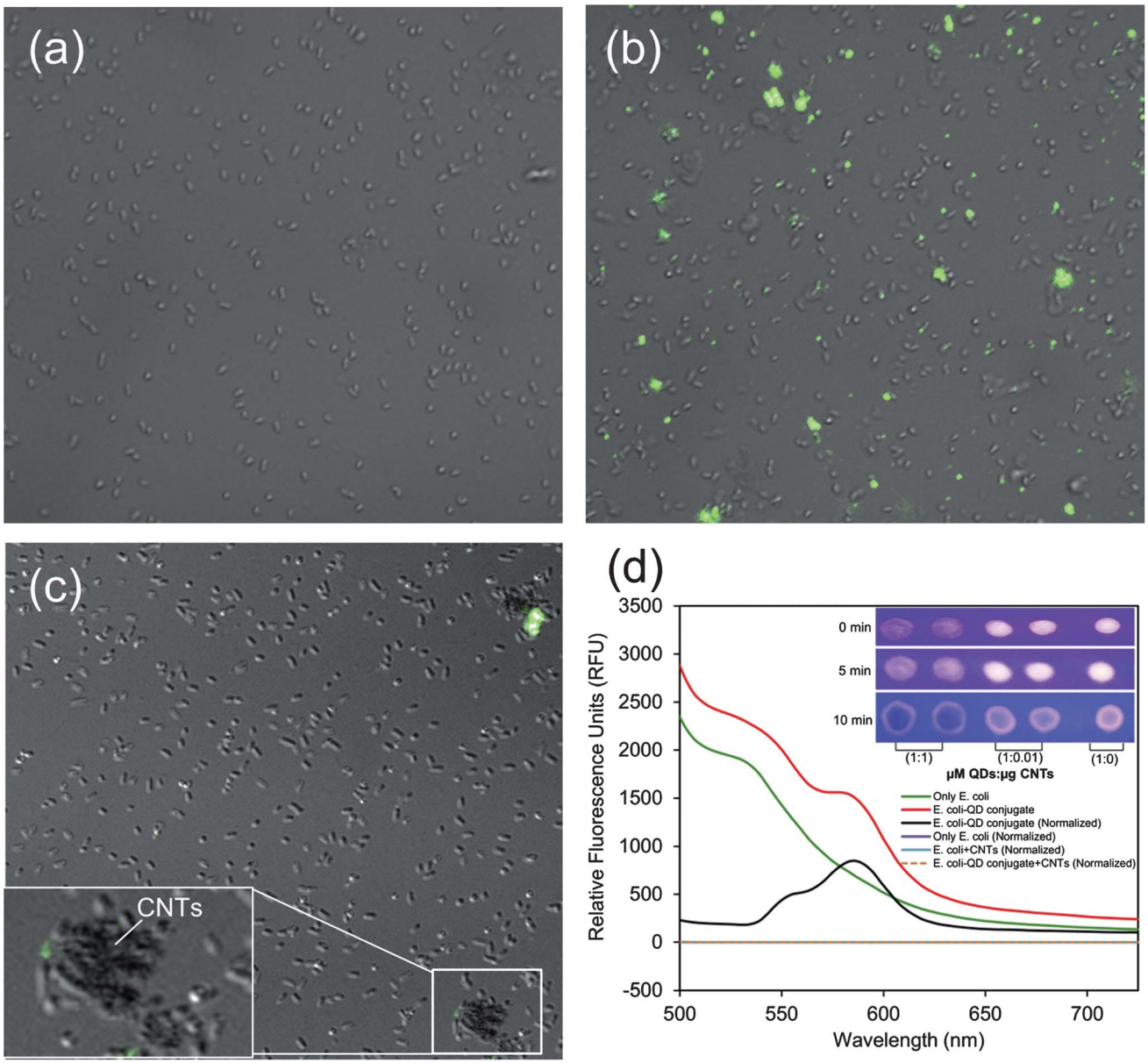

Fig. 3 Confocal microscopic images of *E. coli*–QD bioconjugates taken (a) under normal light, (b) after the laser excitation on *E. coli*–QD bioconjugates and overlayed, (c) loss of fluorescence due to the presence of CNTs after the laser excitation on *E. coli*–QD bioconjugates and (d) fluorescence emission spectra of *E. coli*–QD bioconjugates with or without CNTs incubation showing complete disappearance of fluorescence emission. The fluorescent spectra shown in red and green colors were obtained against PBS as the blank. Normalized curves seen in the spectra were obtained when unlabeled *E. coli* cells were used as control (blank). The inset images show the UV-exposed glass slides spotted with *E. coli*–QD bioconjugates and incubated by mixing with different ratios of CNTs with respect to QDs (QD : CNT = μM : μg) as indicated in the inset legend.

the cellular damage caused by CNTs, mainly by physical injuries to cells, followed by the loss of QDs (Fig. 5a–d).

It is clear from our results as well as those reported earlier[27] that CNTs exhibited detrimental effects on *E. coli* cells. Intracellular trafficking of CNTs occurred individually or in bundles penetrating CNTs through the membrane. Other mechanisms such as phagocytosis have been reported that depend on the cell type, size of nanotube or extent of bundling, and therefore are directly involved in the intracellular trafficking of nanotubes.[27]

The bioassay reported in this study was designed to respond in such a way that any toxic chemical that comes in contact with these cells, either through (a) interaction directly with QDs present on the cell-surface, which quenches the fluorescence emission or (b) its interaction with the cell or cell-membrane damages the cellular integrity which knocks-off the surface bound QDs and thus results in loss of fluorescence emission. The detrimental effects by either of the above two ways caused by NMs or other similar chemicals can be easily probed using whole-cell reporters, such as in this study, *E. coli*–QD bioconjugates through the loss of fluorescence emission or cell viability against CNTs. Therefore, use of these *E.coli*–QD bioconjugates as living cell reporters can provide an important mechanistic perspective for the biological toxicity of NMs similar to CNTs or other xenobiotic chemicals.

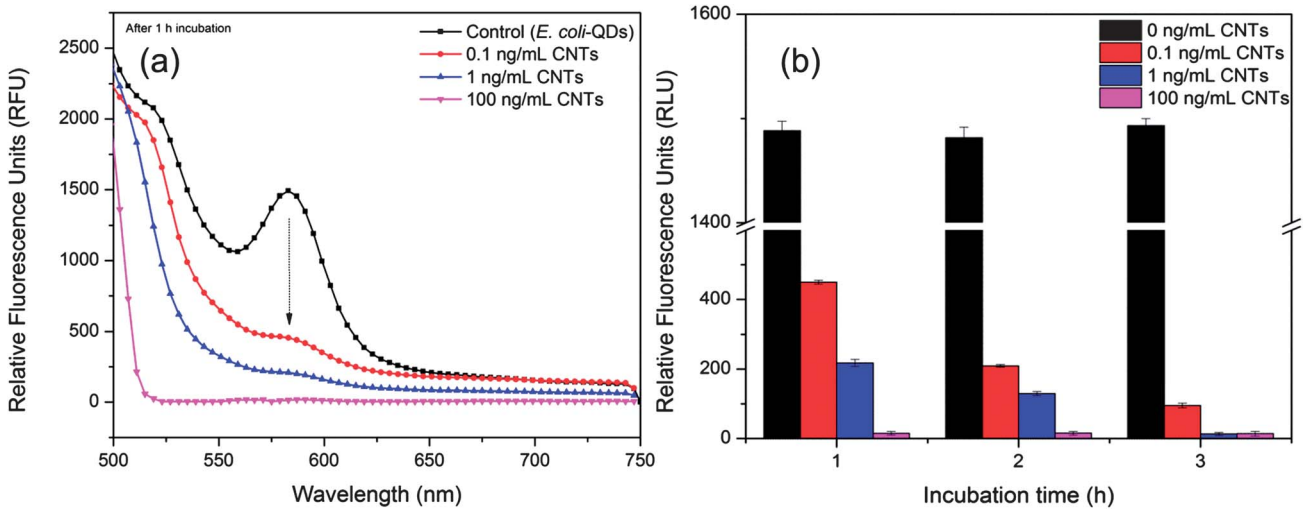

Fig. 4 (a) Fluorescence emission spectra of *E. coli*–QD bioconjugates before and after 1 h incubation with three different concentrations of CNTs indicated in the legend; (b) relative fluorescence units at 585 nm obtained from *E. coli*–QD bioconjugates incubated at different time intervals (1–3 h).

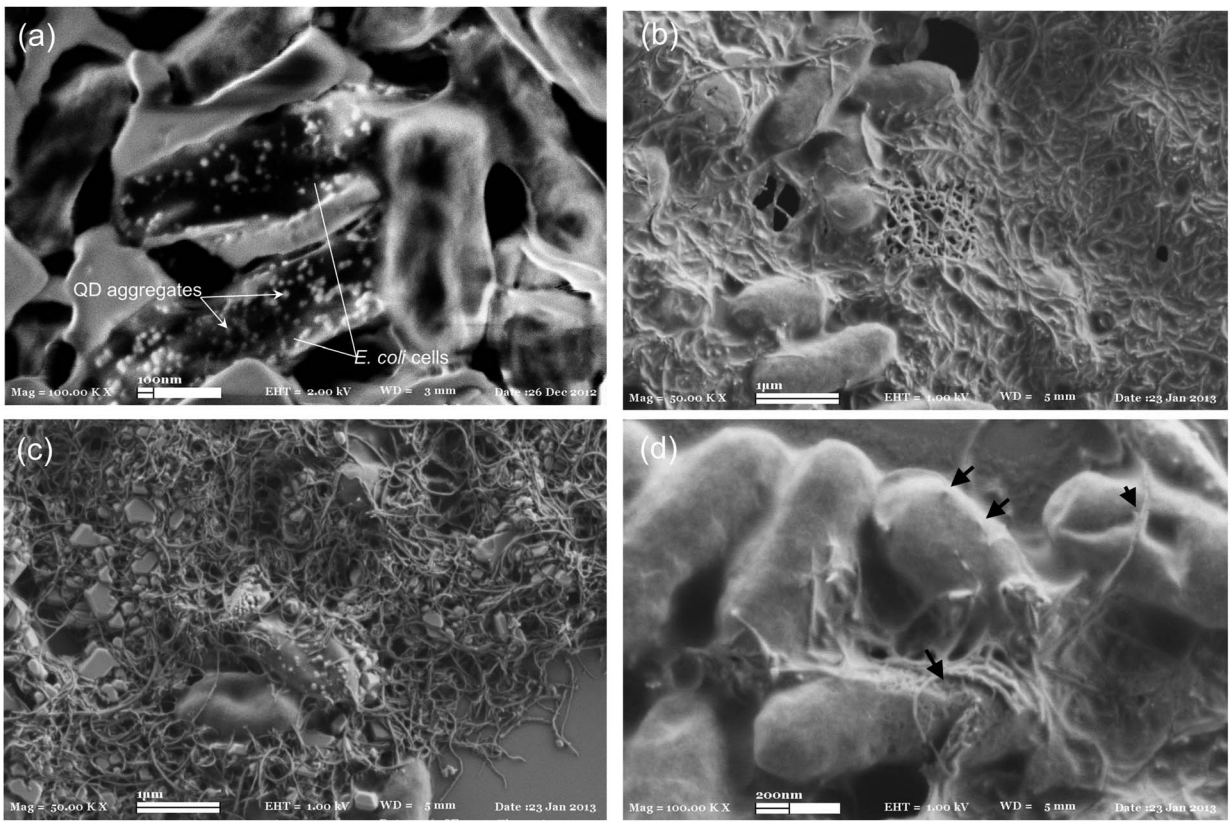

Fig. 5 Scanning electron micrographs of (a) *E. coli*–QD bioconjugates showing QD aggregates, (b) *E. coli*–QD bioconjugates trapped in a mat of CNTs at an initial 1 h incubation, (c) damaged *E. coli*–QD bioconjugates and cellular debris after CNTs were incubated for 3 h and (d) intracellular trafficking of individual or small bundles of CNTs as injecting needles; the arrows indicate specific locations on cells through which CNTs are injected inside the cells.

Conclusions

QDs have emerged as a promising and most exciting NM for electronic materials science to biological applications. In this study, a bioassay was developed to probe the interaction of other NMs, such as CNTs with *E. coli* cells. An *ex vivo* labeling of QDs on *E. coli* cells was performed to develop a whole-cell fluorescent biosensor. QD-labeling was done covalently on the cell-surface without affecting the viability of cells so as to use them as whole-cell biological reporters. The basic mechanism was based on the fluorescent nature of *E. coli*–QD bioconjugates that remain turned on under normal conditions. When a toxic chemical

comes in contact with *E. coli*–QD bioconjugates, their fluorescent behavior is altered or turned-off because of the stress imposed by the toxic chemical. This stress could occur due to many possibilities that arise as a result of interaction of chemicals with the cell-wall or cell membrane and therefore cellular damage occurs. Here, we used CNTs as a model NM and tested their interaction with *E. coli*–QD bioconjugates as whole-cell fluorescent biosensors. Our results demonstrated that the fluorescent ability of these bioconjugates diminishes with time as the CNTs interacted with *E. coli*–QD conjugates that turned off the fluorescence emission from the cells (signal-off mode) because of the possible quenching and/or damaging effects of CNTs. The strategy reported in this study may be useful for creating a novel methodology for investigating cellular interactions with toxic chemicals or ENMs, and the quenching phenomenon of *E. coli*–QD bioconjugates can be used as a new platform to develop a variety of similar fluorescence whole-cell based biosensors.

Acknowledgements

This work was supported by the Scientific and Technological Research Council of Turkey (TUBITAK), project grant no. 112E051. We thank Drs H. Unal and Musa M. Can for helping with confocal microscopy and scanning electron microscopy, respectively.

Notes and references

1 Y. Q. Li, J. H. Wang, H. L. Zhang, J. Yang, L. Y. Guan, H. Chen, Q. M. Luo and Y. D. Zhao, *Biosens. Bioelectron.*, 2010, **25**, 1283–1289.
2 J. F. Weng, X. T. Song, L. A. Li, H. F. Qian, K. Y. Chen, X. M. Xu, C. X. Cao and J. C. Ren, *Talanta*, 2006, **70**, 397–402.
3 P. K. Bae, K. N. Kim, S. J. Lee, H. J. Chang, C. K. Lee and J. K. Park, *Biomaterials*, 2009, **30**, 836–842.
4 Y. He, Y. Y. Su, X. B. Yang, Z. H. Kang, T. T. Xu, R. Q. Zhang, C. H. Fan and S. T. Lee, *J. Am. Chem. Soc.*, 2009, **131**, 4434–4438.
5 L. P. Chen, Z. H. Sheng, A. D. Zhang, X. B. Guo, J. K. Li, H. Y. Han and M. L. Jin, *Luminescence*, 2010, **25**, 419–423.
6 J. V. Jokerst, A. Raamanathan, N. Christodoulides, P. N. Floriano, A. A. Pollard, G. W. Simmons, J. Wong, C. Gage, W. B. Furmaga, S. W. Redding and J. T. McDevitt, *Biosens. Bioelectron.*, 2009, **24**, 3622–3629.
7 Y. Q. Li, L. Y. Guan, J. H. Wang, H. L. Zhang, J. Chen, S. Lin, W. Chen and Y. D. Zhao, *Biosens. Bioelectron.*, 2011, **26**, 2317–2322.
8 X. Y. Wu, H. J. Liu, J. Q. Liu, K. N. Haley, J. A. Treadway, J. P. Larson, N. F. Ge, F. Peale and M. P. Bruchez, *Nat. Biotechnol.*, 2003, **21**, 41–46.
9 H. Ding, K. T. Yong, W. C. Law, I. Roy, R. Hu, F. Wu, W. W. Zhao, K. Huang, F. Erogbogbo, E. J. Bergey and P. N. Prasad, *Nanoscale*, 2011, **3**, 1813–1822.
10 C. Hoffmann, A. C. Faure, C. Vancaeyzeele, S. Roux, O. Tillement, E. Pauthe and F. Goubard, *Anal. Bioanal. Chem.*, 2011, **399**, 1653–1663.
11 J. Kang, X. Y. Zhang, L. D. Sun and X. X. Zhang, *Talanta*, 2007, **71**, 1186–1191.
12 L. Trapiella-Alfonso, J. M. Costa-Fernandez, R. Pereiro and A. Sanz-Medel, *Biosens. Bioelectron.*, 2011, **26**, 4753–4759.
13 C. Gerhards, C. Schulz-Drost, V. Sgobba and D. M. Guldi, *J. Phys. Chem. B*, 2008, **112**, 14482–14491.
14 J. B. Delehanty, C. E. Bradburne, K. Boeneman, K. Susumu, D. Farrell, B. C. Mei, J. B. Blanco-Canosa, G. Dawson, P. E. Dawson, H. Mattoussi and I. L. Medintz, *Integr. Biol.*, 2010, **2**, 265–277.
15 T. Pons, I. L. Medintz, X. Wang, D. S. English and H. Mattoussi, *J. Am. Chem. Soc.*, 2006, **128**, 15324–15331.
16 A. K. Shakya, H. Sami, A. Srivastava and A. Kumar, *Prog. Polym. Sci.*, 2010, **35**, 459–486.
17 I. L. Medintz, E. R. Goldman, M. E. Lassman and J. M. Mauro, *Bioconjugate Chem.*, 2003, **14**, 909–918.
18 C. F. Jones and D. W. Grainger, *Adv. Drug Delivery Rev.*, 2009, **61**, 438–456.
19 A. M. Thayer, *Carbon*, 2007, **85**, 29–35.
20 W. Hannah and P. B. Thompson, *J. Environ. Monit.*, 2008, **10**, 291–300.
21 R. E. Hester and R. M. Harrison, *Nanotechnology: consequences for human health and the environment*, Royal Society of Chemistry, 2007.
22 R. N. Seetharam and K. R. Sridhar, *Curr. Sci.*, 2007, **93**, 769–770.
23 J. L. Ramos, T. Krell, C. Daniels, A. Segura and E. Duque, *Curr. Opin. Microbiol.*, 2009, **12**, 215–220.
24 J. H. Lee, C. H. Youn, B. C. Kim and M. B. Gu, *Biosens. Bioelectron.*, 2007, **22**, 2223–2229.
25 P. Wick, P. Manser, L. K. Limbach, U. Dettlaff-Weglikowska, F. Krumeich, S. Roth, W. J. Stark and A. Bruinink, *Toxicol. Lett.*, 2007, **168**, 121–131.
26 Y. Zhu, T. C. Ran, Y. G. Li, J. X. Guo and W. X. Li, *Nanotechnology*, 2006, **17**, 4668–4674.
27 K. Kostarelos, L. Lacerda, G. Pastorin, W. Wu, S. Wieckowski, J. Luangsivilay, S. Godefroy, D. Pantarotto, J. P. Briand, S. Muller, M. Prato and A. Bianco, *Nat. Nanotechnol.*, 2007, **2**, 108–113.
28 K. J. Boor, *PLoS Biol.*, 2006, **4**, 18–20.
29 R. S. Chouhan, A. C. Vinayaka and M. S. Thakur, *Anal. Bioanal. Chem.*, 2010, **397**, 1467–1475.
30 M. Hartmann, M. Berditsch, J. Hawecker, M. F. Ardakani, D. Gerthsen and A. S. Ulrich, *Antimicrob. Agents Chemother.*, 2010, **54**, 3132–3142.
31 C. Yang, H. Xie, Y. Li, J. K. Zhang and B. L. Su, *J. Colloid Interface Sci.*, 2013, **393**, 438–444.
32 J. K. Jaiswal, H. Mattoussi, J. M. Mauro and S. M. Simon, *Nat. Biotechnol.*, 2003, **21**, 47–51.
33 M. Grzelczak, M. A. Correa-Duarte, V. Salugueirino-Maceira, M. Giersig, R. Diaz and L. M. Liz-Marzan, *Adv. Mater.*, 2006, **18**, 415–420.
34 D. Pantarotto, R. Singh, D. McCarthy, M. Erhardt, J. P. Briand, M. Prato, K. Kostarelos and A. Bianco, *Angew. Chem., Int. Ed.*, 2004, **43**, 5242–5246.
35 G. Jia, H. F. Wang, L. Yan, X. Wang, R. J. Pei, T. Yan, Y. L. Zhao and X. B. Guo, *Environ. Sci. Technol.*, 2005, **39**, 1378–1383.
36 S. Kang, M. Pinault, L. D. Pfefferle and M. Elimelech, *Langmuir*, 2007, **23**, 8670–8673.

